Stress Around a Shaft or Level Excavated in Ground with a Three-Dimensional Stress State

By

Yoshio HIRAMATSU* and Yukitoshi OKA*

(Received October 31, 1961)

The stress around underground openings is much affected by the state of stress in the ground at which the opening is made. The present paper describes the results of an investigation of the stress distributions around a vertical shaft, an inclined shaft and a level, taking into account the fact that the ground is in a three-dimensional stress state.

First the stress around a circular inclined shaft is analyzed strictly and it is proved that some components of the stress are indeterminate. Secondly the general method of experimental analysis of stress by means of two-dimensional and three-dimensional photoelastic experiments is discussed, paying special attention to the evaluation of indeterminate stresses. By the method thus obtained, the stress is found around a shaft or level with a square or rectangular cross section having rounded corners, from which the influence of the state of stress in the undisturbed ground upon the stress around a shaft or level is discussed.

Introduction

In general, the principal. stresses in the undisturbed ground are not always directed to the vertical and horizontal, and their relative intensity may take several values according to topographical, geological and orogenic conditions. Therefore, in investigating earth pressure phenomena, it is necessary to analyze the stress around underground openings taking into account the fact that the undisturbed ground is generally in a three-dimensional stress state.

Yamaguchi[1] analyzed the stress around a circular level, and Suzuki[2] the stress around a circular shaft. These analyses, however, were carried out under the assumption that the direction of one of the principal stresses in the undisturbed ground coincided with the direction of the axis of the shaft or level. The stress around a circular level has been frequently treated in the literature, but it has always been analyzed as a two-dimensional stress. Sugihara[3] analyzed the stress around an inclined shaft under the assumption that the stress in the undisturbed ground was uniform in all directions.

Recently the authors[4] analyzed the stress around a level with several shapes of cross section excavated in ground in which one of the principal stresses

---

* Department of Mining Engineering

coincided with the axis of the level, while the other two principal stresses took any direction. This assumption about the state of stress in the undisturbed ground, however, is not fully general. Therefore, the authors have attempted to analyze theoretically and experimentally the stress around a vertical or inclined shaft or a level excavated in ground whose state of stress is three-dimensional.

Theoretical Analysis of Stress Around a Circular Shaft or Level

The analyses of stress around a vertical or inclined shaft and around a level come to the same analysis in the general case where the ground in which the excavation is made is in a three-dimensional state of stress. Thus we shall only discuss the analysis of stress around an inclined circular shaft.

Let the principal stresses in the undisturbed ground be p_1, p_2 and p_3 and the angle of inclination of the axis ST of an inclined shaft be ϕ. Take two systems of rectangular coordinates (x, y, z) and (x', y', z'), with the same origin 0 on ST. As shown in Fig. 1, the z–axis is vertical, the x–axis coincides with the horizontal projection of ST and the y–axis is perpendicular to both x and z–axes, while x', y' and z'–axes are defined in the directions of p_1, p_2 and p_3 respectively. Further, let us take cylindrical coordinates (r, θ, ζ), whose origin, initial line and ζ–axis coincide with Point 0, the y–axis and ST respectively.
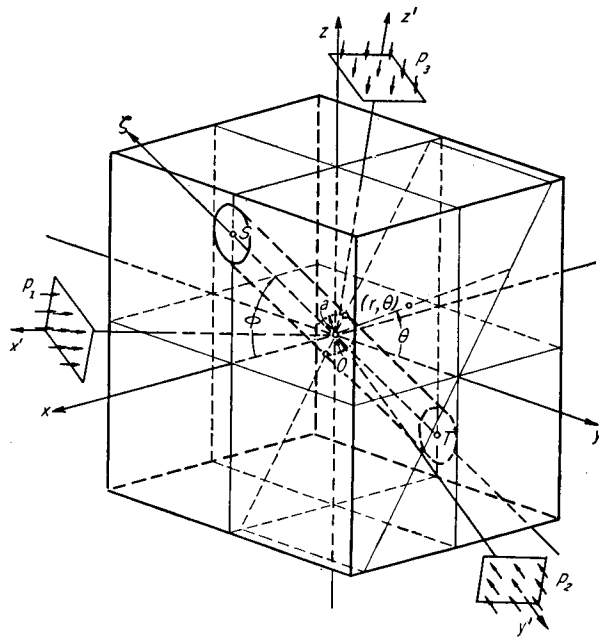

Fig. 1.

Now, the conditions of equilibrium of forces are expressed, in cylindrical coordinates, as:

$$\frac{\partial \sigma_r}{\partial r} + \frac{1}{r}\frac{\partial \tau_{r\theta}}{\partial \theta} + \frac{\partial \tau_{\zeta r}}{\partial \zeta} + \frac{\sigma_r - \sigma_\theta}{r} = 0,$$

$$\frac{\partial \tau_{r\theta}}{\partial r} + \frac{1}{r}\frac{\partial \sigma_\theta}{\partial \theta} + \frac{\partial \tau_{\theta\zeta}}{\partial \zeta} + 2\frac{\tau_{r\theta}}{r} = 0, \qquad (1.1)$$

$$\frac{\partial \tau_{\zeta r}}{\partial r} + \frac{1}{r}\frac{\partial \tau_{\theta\zeta}}{\partial \theta} + \frac{\partial \sigma_\zeta}{\partial \zeta} + \frac{\tau_{\zeta r}}{r} = 0.$$

in which σ_r, σ_θ, σ_ζ, $\tau_{\theta\zeta}$, $\tau_{\zeta r}$ and $\tau_{r\theta}$ are components of stress referring to (r, θ, ζ) coordinates*. In elastic bodies, there exist the following relations between components of stress and components of strain.

$$
\left.
\begin{aligned}
\sigma_r &= \lambda e + 2\mu \frac{\partial u}{\partial r}, \\
\sigma_\theta &= \lambda e + 2\mu \left(\frac{1}{r} \frac{\partial v}{\partial \theta} + \frac{u}{r} \right), \\
\sigma_\zeta &= \lambda e + 2\mu \frac{\partial w}{\partial \zeta}, \\
\tau_{\theta\zeta} &= \mu \left(\frac{1}{r} \frac{\partial w}{\partial \theta} + \frac{\partial v}{\partial \zeta} \right), \\
\tau_{\zeta r} &= \mu \left(\frac{\partial u}{\partial \zeta} + \frac{\partial w}{\partial r} \right), \\
\tau_{r\theta} &= \mu \left(\frac{\partial v}{\partial r} - \frac{v}{r} + \frac{1}{r} \frac{\partial u}{\partial \theta} \right),
\end{aligned}
\right\}
\tag{1.2}
$$

in which λ and μ are Lamé's constants, and u, v and w are the components of displacement in the directions of the radius vector, perpendicular to both the the radius vector and ζ-axis and of ζ-axis respectively, and e is the volumetric strain given by

$$
e = \frac{u}{r} + \frac{\partial u}{\partial r} + \frac{1}{r} \frac{\partial v}{\partial \theta} + \frac{\partial w}{\partial \zeta} .
\tag{1.3}
$$

Since all the components of stress and two of the three components of displacement, u and v, as well as the component of strain in the direction of ζ-axis, $(\varepsilon)_\zeta$, do not vary with ζ, Eqs. (1.1), (1.2) and (1.3) are simplified as follows:

$$
\left.
\begin{aligned}
\frac{\partial \sigma_r}{\partial r} + \frac{1}{r} \frac{\partial \tau_{r\theta}}{\partial \theta} + \frac{\sigma_r - \sigma_\theta}{r} &= 0, \\
\frac{\partial \tau_{r\theta}}{\partial r} + \frac{1}{r} \frac{\partial \sigma_\theta}{\partial \theta} + 2 \frac{\tau_{r\theta}}{r} &= 0, \\
\frac{\partial \tau_{\zeta r}}{\partial r} + \frac{1}{r} \frac{\partial \tau_{\theta\zeta}}{\partial \theta} + \frac{\tau_{\zeta r}}{r} &= 0,
\end{aligned}
\right\}
\tag{1.4}
$$

$$
\sigma_r = \lambda e + 2\mu \frac{\partial u}{\partial r},
\tag{1.5-a}
$$

$$
\sigma_\theta = \lambda e + 2\mu \left(\frac{1}{r} \frac{\partial v}{\partial \theta} + \frac{u}{r} \right),
\tag{1.5-b}
$$

$$
\sigma_\zeta = \lambda e + 2\mu K,
\tag{1.5-c}
$$

$$
\tau_{\theta\zeta} = \mu \frac{1}{r} \frac{\partial w}{\partial \theta},
\tag{1.5-d}
$$

---

* Eq. (1.1) is deduced neglecting the body force, but it may be justified so long as the section of ground concerned is not very shallow.

$$\tau_{\zeta r} = \mu \frac{\partial w}{\partial r}, \tag{1.5-e}$$

$$\tau_{r\theta} = \mu \left(\frac{\partial v}{\partial r} - \frac{v}{r} + \frac{1}{r} \frac{\partial u}{\partial \theta} \right), \tag{1.5-f}$$

$$e = \frac{u}{r} + \frac{\partial u}{\partial r} + \frac{1}{r} \frac{\partial v}{\partial \theta} + K, \tag{1.6}$$

in which $\qquad\qquad K = (\varepsilon)_\zeta = \dfrac{\partial w}{\partial \zeta} = \text{const.}$

Substituting Eqs. (1.5) and (1.6) for σ_r, $\sigma_{\zeta\theta}$, σ_ζ, $\tau_{\theta\zeta}$, $\tau_{\zeta r}$ and $\tau_{r\theta}$ in Eq. (1.4),

$$(\lambda + \mu) \frac{\partial e}{\partial r} + \mu \left(\frac{\partial^2 u}{\partial r^2} + \frac{1}{r} \frac{\partial u}{\partial r} - \frac{u}{r^2} + \frac{1}{r^2} \frac{\partial^2 u}{\partial \theta^2} - \frac{2}{r^2} \frac{\partial v}{\partial \theta} \right) = 0, \tag{1.7-a}$$

$$(\lambda + \mu) \frac{1}{r} \frac{\partial e}{\partial \theta} + \mu \left(\frac{\partial^2 v}{\partial r^2} + \frac{1}{r} \frac{\partial v}{\partial r} - \frac{v}{r^2} + \frac{1}{r^2} \frac{\partial^2 v}{\partial \theta^2} + \frac{2}{r^2} \frac{\partial u}{\partial \theta} \right) = 0, \tag{1.7-b}$$

$$\frac{\partial^2 w}{\partial r^2} + \frac{1}{r} \frac{\partial w}{\partial r} + \frac{1}{r^2} \frac{\partial^2 w}{\partial \theta^2} = 0. \tag{1.7-c}$$

As the boundary conditions, we have:
for large values of r,

$$\left. \begin{array}{l} \sigma_{x'} = p_1, \quad \sigma_{y'} = p_2, \quad \sigma_{z'} = p_3, \\ \tau_{y'z'} = \tau_{z'x'} = \tau_{x'y'} = 0, \end{array} \right\} \tag{1.8}$$

and for $r = a$ (=radius of an inclined shaft),

$$\sigma_r = 0, \tag{1.9-a}$$

$$\tau_{\zeta r} = 0, \tag{1.9-b}$$

$$\tau_{r\theta} = 0. \tag{1.9-c}$$

Now, let us represent the boundary condition (1.8) in terms of components of stress referred to (r, θ, ζ) coordinates. Assume that the direction cosines of x', y' and z'-axes are l_1, l_2, l_3; m_1, m_2, m_3 and n_1, n_2, n_3 respectively. Then,

$$\left. \begin{array}{l} \sigma_x = l_1^2 \sigma_{x'} + m_1^2 \sigma_{y'} + n_1^2 \sigma_{z'} + 2m_1 n_1 \tau_{y'z'} + 2n_1 l_1 \tau_{z'x'} + 2l_1 m_1 \tau_{x'y'}, \\ \sigma_y = l_2^2 \sigma_{x'} + m_2^2 \sigma_{y'} + n_2^2 \sigma_{z'} + 2m_2 n_2 \tau_{y'z'} + 2n_2 l_2 \tau_{z'x'} + 2l_2 m_2 \tau_{x'y'}, \\ \sigma_z = l_3^2 \sigma_{x'} + m_3^2 \sigma_{y'} + n_3^2 \sigma_{z'} + 2m_3 n_3 \tau_{y'z'} + 2n_3 l_3 \tau_{z'x'} + 2l_3 m_3 \tau_{x'y'}, \\ \tau_{yz} = l_2 l_3 \sigma_{x'} + m_2 m_3 \sigma_{y'} + n_2 n_3 \sigma_{z'} + (m_2 n_3 + n_2 m_3) \tau_{y'z'} + (n_2 l_3 + l_2 n_3) \tau_{z'x'} \\ \qquad + (l_2 m_3 + m_2 l_3) \tau_{x'y'}, \\ \tau_{zx} = l_3 l_1 \sigma_{x'} + m_3 m_1 \sigma_{y'} + n_3 n_1 \sigma_{z'} + (m_3 n_1 + n_3 m_1) \tau_{y'z'} + (n_3 l_1 + l_3 n_1) \tau_{z'x'} \\ \qquad + (l_3 m_1 + m_3 l_1) \tau_{x'y'}, \\ \tau_{xy} = l_1 l_2 \sigma_{x'} + m_1 m_2 \sigma_{y'} + n_1 n_2 \sigma_{z'} + (m_1 n_2 + n_1 m_2) \tau_{y'z'} + (n_1 l_2 + l_1 n_2) \tau_{z'x'} \\ \qquad + (l_1 m_2 + m_1 l_2) \tau_{x'y'}. \end{array} \right\} \tag{1.10}$$

Substituting Eq. (1.8) for $\sigma_{x'}$, $\sigma_{y'}$, $\cdots$, $\tau_{x'y'}$ in Eq. (1.10),

$$\sigma_x = l_1^2 p_1 + m_1^2 p_2 + n_1^2 p_3 \,,$$
$$\sigma_y = l_2^2 p_1 + m_2^2 p_2 + n_2^2 p_3 \,,$$
$$\sigma_z = l_3^2 p_1 + m_3^2 p_2 + n_3^2 p_3 \,,$$
$$\tau_{yz} = l_2 l_3 p_1 + m_2 m_3 p_2 + n_2 n_3 p_3 \,,$$
$$\tau_{zx} = l_3 l_1 p_1 + m_3 m_1 p_2 + n_3 n_1 p_3 \,,$$
$$\tau_{xy} = l_1 l_2 p_1 + m_1 m_2 p_2 + n_1 n_2 p_3 \,.$$

(1.11)

From geometry,

$$\cos(x, r) = -\sin\phi\sin\theta \,, \quad \cos(x, \theta) = -\sin\phi\cos\theta \,, \quad \cos(x, \zeta) = \cos\phi \,,$$
$$\cos(y, r) = \cos\theta \,, \qquad\qquad \cos(y, \theta) = -\sin\theta \,, \qquad \cos(y, \zeta) = 0 \,,$$
$$\cos(z, r) = \cos\phi\sin\theta \,, \quad \cos(z, \theta) = \cos\phi\cos\theta \,, \qquad \cos(z, \zeta) = \sin\phi \,.$$

(1.12)

Transforming the components of stress from (x, y, z) coordinates into those of (r, θ, ζ) coordinates, and considering Eq. (1.11), we have:

$$\sigma_r = \alpha_1 + \alpha_2 \cos 2\theta + \alpha_3 \sin 2\theta \,,$$ (1.13-a)

$$\sigma_\theta = \alpha_1 - \alpha_2 \cos 2\theta - \alpha_3 \sin 2\theta \,,$$ (1.13-b)

$$\sigma_\zeta = \beta_1 ,$$ (1.13-c)

$$\tau_{\theta\zeta} = \gamma_1 \cos\theta + \gamma_2 \sin\theta \,,$$ (1.13-d)

$$\tau_{\zeta r} = \gamma_1 \sin\theta - \gamma_2 \cos\theta \,,$$ (1.13-e)

$$\tau_{r\theta} = -\alpha_2 \sin 2\theta + \alpha_3 \cos 2\theta \,,$$ (1.13-f)

in which

$$\alpha_1 = \frac{1}{2}\{(l_1^2 \sin^2\phi + l_2^2 + l_3^2 \cos^2\phi - 2l_3 l_1 \sin\phi\cos\phi)p_1$$
$$+ (m_1^2 \sin^2\phi + m_2^2 + m_3^2 \cos^2\phi - 2m_3 m_1 \sin\phi\cos\phi)p_2$$
$$+ (n_1^2 \sin^2\phi + n_2^2 + n_3^2 \cos^2\phi - 2n_3 n_1 \sin\phi\cos\phi)p_3\} \,,$$

$$\alpha_2 = \frac{1}{2}\{(-l_1^2 \sin^2\phi + l_2^2 - l_3^2 \cos\phi + 2l_3 l_1 \sin\phi\cos\phi)p_1$$
$$+ (-m_1^2 \sin^2\phi + m_2^2 - m_3^2 \cos^2\phi + 2m_3 m_1 \sin\phi\cos\phi)p_2$$
$$+ (-n_1^2 \sin^2\phi + n_2^2 - n_3^2 \cos^2\phi + 2n_3 n_1 \sin\phi\cos\phi)p_3\} \,,$$

$$\alpha_3 = (l_2 l_3 \cos\phi - l_1 l_2 \sin\phi)p_1 + (m_2 m_3 \cos\phi - m_1 m_2 \sin\phi)p_2$$
$$+ (n_2 n_3 \cos\phi - n_1 n_2 \sin\phi)p_3 \,,$$

$$\beta_1 = (l_1^2 \cos^2\phi + l_3^2 \sin^2\phi + 2l_3 l_1 \sin\phi\cos\phi)p_1$$
$$+ (m_1^2 \cos^2\phi + m_3^2 \sin^2\phi + 2m_3 m_1 \sin\phi\cos\phi)p_2$$
$$+ (n_1^2 \cos^2\phi + n_3^2 \sin^2\phi + 2n_3 n_1 \sin\phi\cos\phi)p_3 \,,$$

$$\gamma_1 = \{-l_1^2 \sin\phi\cos\phi + l_3^2 \cos\phi\sin\phi + l_3 l_1(\cos^2\phi - \sin^2\phi)\}p_1$$
$$+ \{-m_1^2 \sin\phi\cos\phi + m_3^2 \cos\phi\sin\phi + m_3 m_1(\cos^2\phi - \sin^2\phi)\}p_2$$
$$+ \{-n_1^2 \sin\phi\cos\phi + n_3^2 \cos\phi\sin\phi + n_3 n_1(\cos^2\phi - \sin\phi)\}p_3 \,,$$

$$\gamma_2 = (-l_2 l_3 \sin\phi - l_1 l_2 \cos\phi)p_1 + (-m_2 m_3 \sin\phi - m_1 m_2 \cos\phi)p_2$$
$$+ (-n_2 n_3 \sin\phi - n_1 n_2 \cos\phi)p_3 \,.$$

(1.14)

Eq. (1.13) is the substitute of Eq. (1.18). Solving Eq. (1.7-c) for w, and considering Eqs. (1.5-d), (1.5-e), (1.13-d) and (1.13-e), we obtain

$$w = (A_1'r + A_1 r^{-1}) \cos \theta + (B_1'r + B_1 r^{-1}) \sin \theta . \tag{1.15}$$

Consequently, from Eqs. (1.2-d) and (1.2-e), we have

$$\tau_{\theta\zeta} = \mu\{(-A_1' - A_1 r^{-2}) \sin \theta + (B_1' + B_1 r^{-2}) \cos \theta\} ,$$
$$\tau_{\zeta r} = \mu\{(A_1' - A_1 r^{-2}) \cos \theta + (B_1' - B_1 r^{-2}) \sin \theta\} .$$

From Eqs. (1.13-d), (1.13-e) and (1.9-b),

$$\tau_{\theta\zeta} = \gamma_1\left(1 + \frac{a^2}{r^2}\right) \cos \theta + \gamma_2\left(1 + \frac{a^2}{r^2}\right) \sin \theta , \tag{1.16}$$

$$\tau_{\zeta r} = \gamma_1\left(1 - \frac{a^2}{r^2}\right) \sin \theta - \gamma_2\left(1 - \frac{a^2}{r^2}\right) \cos \theta . \tag{1.17}$$

Eqs. (1.7-a) and (1.7-b) are rewritten as:

$$(\lambda + 2\mu)\frac{\partial e}{\partial r} + \mu\left(\frac{1}{r^2}\frac{\partial^2 u}{\partial \theta^2} - \frac{1}{r^2}\frac{\partial v}{\partial \theta} - \frac{1}{r}\frac{\partial^2 v}{\partial r\partial \theta}\right) = 0 , \tag{1.18-a}$$

$$(\lambda + 2\mu)\frac{1}{r}\frac{\partial e}{\partial \theta} + \mu\left(\frac{\partial^2 v}{\partial r^2} + \frac{1}{r}\frac{\partial v}{\partial r} - \frac{v}{r^2} + \frac{1}{r^2}\frac{\partial u}{\partial \theta} + \frac{1}{r}\frac{\partial^2 u}{\partial r\partial \theta}\right) = 0 . \tag{1.18-b}$$

Differentiate Eq. (1.18-a) with respect to r and divide the same equation by r. On the other hand, differentiate Eq. (1.18-b) with respect to θ and further divide the result by r. Then by adding these three equations, we obtain

$$\frac{\partial^2 e}{\partial r^2} + \frac{1}{r}\frac{\partial e}{\partial r} + \frac{1}{r^2}\frac{\partial^2 e}{\partial \theta^2} = 0 . \tag{1.19}$$

Considering Eqs. (1.5-a), (1.5-b), (1.5-c), (1.13-a), (1.13-b) (1.13-c) and (1.9-a), Eq. (1.19) is solved as

$$e = C_0 + C_2 r^{-2} \cos 2\theta + D_2 r^{-2} \sin 2\theta . \tag{1.20}$$

Eliminating $\dfrac{\partial e}{\partial r}$ and $\dfrac{\partial v}{\partial \theta}$ by introduction of Eqs. (1.20) and (1.6) to Eq. (1.7-a),

$$\frac{\partial^2 u}{\partial r^2} + \frac{3}{r}\frac{\partial u}{\partial r} + \frac{u}{r^2} + \frac{1}{r^2}\frac{\partial^2 u}{\partial \theta^2}$$
$$= 2(C_0 - K)r^{-1} + \frac{2(\lambda + 2\mu)}{\mu} r^{-3}(C_2 \cos 2\theta + D_2 \sin 2\theta) . \tag{1.21}$$

Solving Eq. (1.21) under consideration of Eqs. (1.5-a), (1.13-a) and (1.9-a),

$$u = 2(C_0 - K)r + E_0 r^{-1} + \left(E_2'r + E_2 r^{-3} - \frac{1}{2}\frac{\lambda + 2\mu}{\mu}C_2 r^{-1}\right) \cos 2\theta$$
$$+ \left(F_2'r + F_2 r^{-3} - \frac{1}{2}\frac{\lambda + 2\mu}{\mu}D_2 r^{-1}\right) \sin 2\theta . \tag{1.22}$$

From Eqs. (1.6), (1.20) and (1.22),

$$\frac{\partial v}{\partial \theta} = er - u - r\frac{\partial u}{\partial r}$$

$$= (-2E_2'r + 2E_2r^{-3} + C_2r^{-1})\cos 2\theta + (-2F_2'r + 2F_2r^{-3} + D_2r^{-1})\sin 2\theta . \quad (1.23)$$

Solving Eq. (1.23) under consideration of Eq. (1.7-b),

$$v = \left(-E_2'r + E_2r^{-3} + \frac{1}{2}C_2r^{-1}\right)\sin 2\theta - \left(-F_2'r + F_2r^{-3} + \frac{1}{2}D_2r^{-1}\right)\cos 2\theta . \quad (1.24)$$

Introducing Eqs. (1.20), (1.22) and (1,24) into Eqs. (1.5-a), (1.5-b), (1.5-c) and (1.5-f), and determining each constant from the boundary conditions represented by Eqs. (1.13-a), (1.13-b), (1.13-c), (1.13-f), (1.19-a) and (1.9-c), we obtain the equations that give the components of stress around a circular inclined shaft as follows:

$$
\left.
\begin{aligned}
\sigma_r &= \alpha_1\left(1 - \frac{a^2}{r^2}\right) + \alpha_2\left(1 - 4\frac{a^2}{r^2} + 3\frac{a^4}{r^4}\right)\cos 2\theta \\
&\quad + \alpha_3\left(1 - 4\frac{a^2}{r^2} + 3\frac{a^4}{r^4}\right)\sin 2\theta , \\
\sigma_\theta &= \alpha_1\left(1 + \frac{a^2}{r^2}\right) + \alpha_2\left(-1 - 3\frac{a^4}{r^4}\right)\cos 2\theta + \alpha_3\left(-1 - 3\frac{a^4}{r^4}\right)\sin 2\theta , \\
\sigma_\zeta &= \beta_1 - \frac{2\lambda}{\lambda + \mu}\alpha_2\frac{a^2}{r^2}\cos 2\theta - \frac{2\lambda}{\lambda + \mu}\alpha_3\frac{a^2}{r^2}\sin 2\theta , \\
\tau_{\theta\zeta} &= \gamma_1\left(1 + \frac{a^2}{r^2}\right)\cos\theta + \gamma_2\left(1 + \frac{a^2}{r^2}\right)\sin\theta , \\
\tau_{\zeta r} &= \gamma_1\left(1 - \frac{a^2}{r^2}\right)\sin\theta - \gamma_2\left(1 - \frac{a^2}{r^2}\right)\cos\theta , \\
\tau_{r\theta} &= \alpha_2\left(-1 - 2\frac{a^2}{r^2} + 3\frac{a^4}{r^4}\right)\sin 2\theta + \alpha_3\left(1 + 2\frac{a^2}{r^2} - 3\frac{a^4}{r^4}\right)\cos 2\theta .
\end{aligned}
\right\} \quad (1.25)
$$

Since Poisson's number m is equal to $2(\lambda + \mu)/\lambda$, $2\lambda/(\lambda + \mu)$ in the third equation of Eq. (1.25) can be replaced by $4/m$. By putting $\phi = 0°$ or $90°$, Eq. (1.25) gives the components of stress around a circular level or vertical shaft.

It is noticed, in Eq. (1.25), that σ_r, σ_θ, $\tau_{\theta\zeta}$, $\tau_{\zeta r}$ and $\tau_{r\theta}$ are independent of elastic constants and therefore determinate, but that σ_ζ depends upon Poisson's number and is therefore indeterminate.

In the case where the direction of one of the principal stresses in the undisturbed ground is assumed to have the same direction as the axis of the cylindrical opening, the components of stress σ_r, σ_θ, $\tau_{r\theta}$ have been analyzed by several investigators simply regarding them as plane stresses. The author's strict solution verifies that this simple analysis is justified. However, σ_ζ is not to be obtained from the simple solution.

Experimental Analysis of Stress Around a Shaft or Level

Theoretical considerations

Let us first discuss the general way to determine experimentally the stress around an opening made in ground with a three-dimensional stress state.

Consider two systems of rectangular coordinates (x, y, z) and (x', y', z'), with the same origin 0. The x, y and z–axes are arbitrary and say that the x and y axes are horizontal and the z–axis is vertical, while the x', y' and z'–axes are taken in the directions of the principal stresses p_1, p_2 and p_3 in the undisturbed ground. Let the direction cosines of x', y' and z'–axes be l_1, l_2, l_3; m_1, m_2, m_3 and n_1, n_2, n_3 respectively.

At any point sufficiently far from an opening, there following relations exist:

$$\left.\begin{aligned}
\sigma_{x'} = p_1, \quad \sigma_{y'} = p_2, \quad \sigma_{z'} = p_3, \\
\tau_{y'z'} = \tau_{z'x'} = \tau_{x'y'} = 0,
\end{aligned}\right\} \tag{2.1}$$

in which $\sigma_{x'}, \sigma_{y'}, \cdots, \tau_{x'y'}$ are components of stress in reference to (x', y', z') coordinates. By expressing Eq. (2.1) with components of stress in reference to (x, y, z) coordinates, we obtain

$$\left.\begin{aligned}
\sigma_x &= l_1^2 p_1 + m_1^2 p^2 + n_1^2 p_3, \\
\sigma_y &= l_2^2 p_1 + m_2^2 p_2 + n_2^2 p_3, \\
\sigma_z &= l_3^2 p_1 + m_3^2 p_2 + n_3^2 p_3, \\
\tau_{yz} &= l_2 l_3 p_1 + m_2 m_3 p_2 + n_2 n_3 p_3, \\
\tau_{zx} &= l_3 l_1 p_1 + m_3 m_1 p_2 + n_3 n_1 p_3, \\
\tau_{xy} &= l_1 l_2 p_1 + m_1 m_2 p_2 + n_1 n_2 p_3.
\end{aligned}\right\} \tag{2.2}$$

If a model for photoelastic experiment is loaded simultaneously in the directions of and with the intensities of p_1, p_2 and p_3 respectively, the state of stress expressed by Eq. (2.2) will be reproduced in the model. But it would be a waste of effort and time to make such an experiment for each given set of p_1, p_2 and p_3.

However, in order to determine the components of stress at any point in a model, it is supposed sufficient to make six kinds of experiment for a given shape of
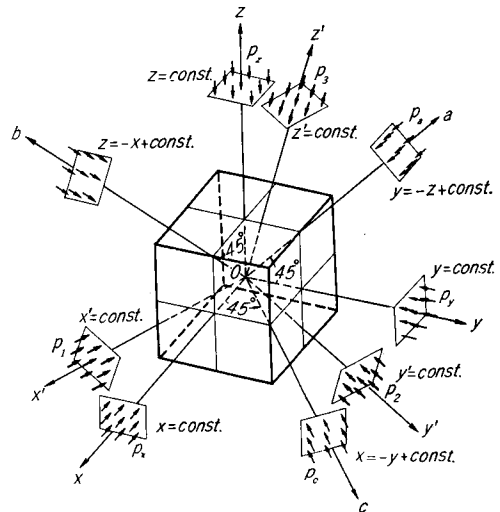

Fig. 2.

opening, whatever the state of stress in the undisturbed ground may be.

Now we shall treat the stress analysis from such experiments where six models are, one by one, loaded in x, y, z, a, b and c-directions with intensities of of p_x, p_y, p_z, p_a, p_b and p_c; the a, b, and c-axes being the bisectors of the y and z-axes, z and x-axes, x and y-axes respectively. (See Fig. 2.) If these six kinds of loading were practiced on a model simultaneously, the components of stress at any point far from the opening would be given by the following equations:

$$\sigma_x = p_x + p_b \cos^2 \frac{\pi}{4} + p_c \cos^2 \frac{\pi}{4} = p_x + \frac{1}{2}(p_b + p_c) , \qquad (2.3\text{-a})$$

$$\sigma_y = p_y + \frac{1}{2}(p_c + p_a) , \qquad (2.3\text{-b})$$

$$\sigma_z = p_z + \frac{1}{2}(p_a + p_b) , \qquad (2.3\text{-c})$$

$$\tau_{yz} = \frac{1}{2} p_a , \quad \tau_{zx} = \frac{1}{2} p_b , \quad \tau_{xy} = \frac{1}{2} p_c . \qquad (2.4)$$

In order that the components of stress given by Eqs. (2.3), and (2.4) become equal to those given by Eq. (2.2), the following relations must exist:

$$\left.\begin{aligned}
p_x + \frac{1}{2}(p_b + p_c) &= l_1^2 p_1 + m_1^2 p_2 + n_1^2 p_3 , \\
p_y + \frac{1}{2}(p_c + p_a) &= l_2^2 p_1 + m_2^2 p_2 + n_2^2 p_3 , \\
p_z + \frac{1}{2}(p_a + p_b) &= l_3^2 p_1 + m_3^2 p_2 + n_3^2 p_3 , \\
\frac{1}{2} p_a &= l_2 l_3 p_1 + m_2 m_3 p_2 + n_2 n_3 p_3 , \\
\frac{1}{2} p_b &= l_3 l_1 p_1 + m_3 m_1 p_2 + n_3 n_1 p_3 , \\
\frac{1}{2} p_c &= l_1 l_2 p_1 + m_1 m_2 p_2 + n_1 n_2 p_3 .
\end{aligned}\right\} \qquad (2.5)$$

Putting

$$\left.\begin{aligned}
\alpha_{1.1} &= l_1^2 - l_3 l_1 - l_1 l_2 , \\
\alpha_{1.2} &= m_1^2 - m_3 m_1 - m_1 m_2 , \\
\alpha_{1.3} &= n_2^2 - n_3 n_1 - n_1 n_2 , \\
\alpha_{2.1} &= l_2^2 - l_1 l_2 - l_2 l_3 , \\
\alpha_{2.2} &= m_2^2 - m_1 m_2 - m_2 m_3 , \\
\alpha_{2.3} &= n_2^2 - n_1 n_2 - n_2 n_3 , \\
\alpha_{3.1} &= l_3^2 - l_2 l_3 - l_3 l_1 , \\
\alpha_{3.2} &= m_3^2 - m_2 m_3 - m_3 m_1 , \\
\alpha_{3.3} &= n_3^2 - n_2 n_3 - n_3 n_1 , \\
\alpha_{4.1} &= 2 l_2 l_3 , \quad \alpha_{4.2} = 2 m_2 m_3 , \quad \alpha_{4.3} = 2 n_2 n_3 ,
\end{aligned}\right\} \qquad (2.6)$$

$$\alpha_{5.1} = 2l_3l_1, \quad \alpha_{5.2} = 2m_3m_1, \quad \alpha_{5.3} = 2n_3n_1, \quad \Big\}$$
$$\alpha_{6.1} = 2l_1l_2, \quad \alpha_{6.2} = 2m_1m_2, \quad \alpha_{6.3} = 2n_1n_2, \quad \Big\}$$

we obtain the following equations.

$$
\left.
\begin{aligned}
p_x &= \alpha_{1.1}p_1 + \alpha_{1.2}p_2 + \alpha_{1.3}p_3, \\
p_y &= \alpha_{2.1}p_1 + \alpha_{2.2}p_2 + \alpha_{2.3}p_3, \\
p_z &= \alpha_{3.1}p_1 + \alpha_{3.2}p_2 + \alpha_{3.3}p_3, \\
p_a &= \alpha_{4.1}p_1 + \alpha_{4.2}p_2 + \alpha_{4.3}p_3, \\
p_b &= \alpha_{5.1}p_1 + \alpha_{5.2}p_2 + \alpha_{5.3}p_3, \\
p_c &= \alpha_{6.1}p_1 + \alpha_{6.2}p_2 + \alpha_{6.3}p_3.
\end{aligned}
\right\}
\tag{2.7}
$$

If a model is loaded by p_x, p_y, p_z, p_a, p_b and p_c simultaneously, the stress state in the model will be just the same as that which is caused by p_1, p_2 and p_3, acting simultaneously.

Now let us explain how to find components of stress expressed in reference to an optional system of coordinates (x'', y'', z'') at any point P in a model, which is loaded by p_1, p_2 and p_3 simultaneously. Six models are prepared, one of which is loaded in the x–direction with an intensity of $\bar{p}_x$, the stress pattern in it being fixed by proper heat treatment. Observing the stress pattern by means of a photoelastic apparatus, the components of stress at Point P are determined, from which the stress coefficients $A_x, B_x, \cdots, F_x$ defined by the following equations are found[*].

$$A_x = (\sigma_{x''})_x/\bar{p}_x, \ B_x = (\sigma_{y''})_x/\bar{p}_x, \cdots, F_x = (\tau_{x''y''})_x/\bar{p}_x, \tag{2.8}$$

in which $(\sigma_{x''})_x$, $(\sigma_{y''})_x$, $\cdots$, $(\tau_{x''y''})_x$ are the components of stress caused by $\bar{p}_x$, expressed in reference to (x'', y'', z'') coordinates.

In the same manner, the other five models are loaded, one by one, by $\bar{p}_y$, $\bar{p}_z$, $\bar{p}_a$, $\bar{p}_b$ and $\bar{p}_c$, and the five groups of stress coefficients $A_y, B_y, \cdots, F_y, \cdots, A_c$, $B_c, \cdots, F_c$ are found.

On the other hand, from given values of p_1, p_2 and p_3, the theoretical intensities of loading p_x, p_y, p_z, p_a, p_b and p_c can be calculated from Eq. (2.7). Thus the components of stress under question are obtained by the following equations.

$$
\left.
\begin{aligned}
\sigma_{x''} &= A_x p_x + A_y p_y + A_z p_z + A_a p_a + A_b p_b + A_c p_c, \\
\sigma_{y''} &= B_x p_x + B_y p_y + B_z p_z + B_a p_a + B_b p_b + B_c p_c, \\
&\quad \cdots\cdots\cdots\cdots \\
&\quad \cdots\cdots\cdots\cdots \\
\tau_{x''y''} &= F_x p_x + F_y p_y + F_z p_z + F_a p_a + F_b p_b + F_c p_c.
\end{aligned}
\right\}
\tag{2.9}
$$

---

[*] In general, the stress around an underground opening is indeterminate. In finding such indeterminate stress by means of three-dimensional photoelastic experiments, one must take a proper measure to meet the fact that the Poisson's number of the material of models decreases down to about 2 when stress patterns are fixed by heat treatment.

Let us proceed to discuss how to determine the stress around a shaft or level with a uniform cross section. In this case the stress analysis becomes far simpler.

It is convenient to take the x-axis along the axis of the shaft or level, the y-axis perpendicular to the x-axis and horizontal, the z-axis perpendicular to both the x and y-axes. Let us explain how to find the components of stress, σ_t, σ_l, τ_{tl} at any given point P on the wall surface, expressed in reference to rectangular coordinates (t, l, n), with origin at Point P, the t-axis being tangent to the wall surface and perpendicular to the x-axis, the l-axis being parallel to the x-axis, and the n-axis being normal to the surface. (See Fig. 3.) Since Point P is on the wall surface,
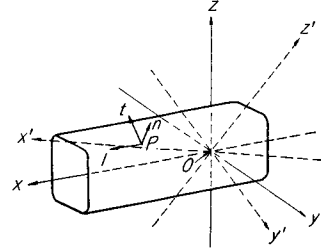

Fig. 3.

$$\sigma_n = \tau_{ln} = \tau_{nt} = 0.$$

The stress coefficients concerning σ_t, σ_l and τ_{tl} shall be denoted by the letters, A, B and F respectively. Now the present problem is to find six groups of stress coefficients, namely:

$$A_x, B_x, F_x; \quad A_y, B_y, F_y; \quad A_z, B_z, F_z;$$
$$A_a, B_a, F_a; \quad A_b, B_b, F_b; \quad A_c, B_c, F_c;$$

from six experiments. However, on theoretical grounds the first group of stress coefficients A_x, B_x and F_x, which are to be determined from an experiment loading a model in the direction of the axis of opening, is given by:

$$A_x = 0, \quad B_x = 1, \quad F_x = 0. \tag{2.10}$$

Therefore the experiment in which a model is loaded in the x-direction can be omitted.

We must pay attention to the fact that we can not determine σ_l from three-dimensional photoelastic experiments. The reason is that, judging from the strict analysis of stress, expressed by Eq. (1.25), around a circular inclined shaft, σ_l depends upon the elastic constants and is indeterminate, while on the other hand Poisson's number for the model material decreases down to almost 2 when the stress pattern is fixed by heat treatment, and accordingly the determination of the indeterminate stress σ_l is impossible from three-dimensional photoelastic experiments.

An alternative method to find σ_l was investigated and developed as follows. Let Young's modulus and Poisson's number of the ground in which a shaft or

level is excavated be E and m respectively, and the strain at Point P in the l-direction be ζ_l. Then, from the relation between stress and strain in an elastic body,

$$(\sigma_l)_y = E(\varepsilon_l)_y + \frac{1}{m}\{(\sigma_t)_y + (\sigma_n)_y\} = E(\varepsilon_l)_y + \frac{1}{m}(\sigma_t)_y,$$

$$(\sigma_l)_z = E(\varepsilon_l)_z + \frac{1}{m}(\sigma_t)_z,$$

$$\cdots\cdots\cdots\cdots\cdots$$
$$\cdots\cdots\cdots\cdots$$

$$(\sigma_l)_c = E(\varepsilon_l)_c + \frac{1}{m}(\sigma_t)_c.$$

On the other hand, by definition we have

$$(\sigma_l)_y = B_y p_y, \quad (\sigma_l)_z = B_z p_z, \cdots, (\sigma_l)_c = B_c p_c,$$
$$(\sigma_t)_y = A_y p_y, \quad (\sigma_t)_z = A_z p_z, \cdots, (\sigma_t)_c = A_c p_c.$$

Hence

$$\left.\begin{aligned}
B_y &= (\varepsilon_l)_y \cdot \frac{E}{p_y} + \frac{A_y}{m}, \\
B_z &= (\varepsilon_l)_z \cdot \frac{E}{p_z} + \frac{A_z}{m}, \\
&\cdots\cdots\cdots \\
B_c &= (\varepsilon_l)_c \cdot \frac{E}{p_c} + \frac{A_c}{m}.
\end{aligned}\right\} \tag{2.11}$$

Since it is supposed that ε_l does not vary upon excavating a shaft or level, we have

$$\left.\begin{aligned}
B_y &= (A_y - 1)/m, \quad && B_z = (A_z - 1)/m, \\
B_a &= (A_a - 1)/m, \quad && B_b = (2A_b + m - 1)/2m, \\
B_c &= (2A_c + m - 1)/2m. &&
\end{aligned}\right\} \tag{2.12}$$

Since σ_t and σ_l can be determined by regarding them as two-dimensional stresses, the three kinds of photoelastic experiment in which models are loaded in the y, z and a-directions are enough to be two-dimensional. Consequently only the two kinds of experiment in which models are loaded in the b and c-direction must be three-dimensional. However, since two-dimensional photoelastic experiments are superior to three-dimensional ones in accuracy, it is preferable to find A_b and A_c from two-dimensional experiments rather than from three-dimensional ones, by means of the following equations*:

---

* Let the $\bar{b}$-axis be the bisector of the y-axis and the minus side of the x-axis. If a model is loaded in the b and $\bar{b}$-directions simultaneously with the same intensity p_b, the components of stress at any point far from the opening are given by

$$\sigma_x = \frac{1}{2}p_b + \frac{1}{2}p_b = p_b, \qquad \sigma_y = 0, \qquad \sigma_z = \frac{1}{2}p_b + \frac{1}{2}p_b = p_b$$

$$\tau_{yz} = 0, \qquad \tau_{zx} = \frac{1}{2}p_b - \frac{1}{2}p_b = 0, \qquad \tau_{xy} = 0.$$

$$A_b = A_z/2, \qquad A_c = A_y/2. \tag{2.13}$$

Making use of this relation, B_a and B_b in Eq. (2.12) can be rewritten as:

$$\left. \begin{array}{l} B_b = (A_z + m - 1)/2m, \\ B_c = (A_y + m - 1)/2m. \end{array} \right\} \tag{2.14}$$

When the cross section of an opening has more than one axis of symmetry, such as a circle, square, rectangle, trapezoid or arch shape, the following relation exists among A_y, A_z and A_a**:

$$A_y + A_z = A_a + \bar{A}_a, \tag{2.15}$$

in which $\bar{A}_a$ is the stress coefficient representing σ_t at the symmetrical point of Point P with respect to the axis of symmetry. It is advisable to improve the accuracy in the determination of A_y, A_z and A_a by making use of Eq. (2.15).

It must be noted that τ_{tl} is always zero when a model is loaded in the x, y, z and a-directions. Therefore

$$F_x = F_y = F_z = F_a = 0. \tag{2.16}$$

In short, the components of stress at the wall surface of a vertical or inclined shaft or a level can be obtained from the following equations:

$$\left. \begin{array}{l} \sigma_t = A_y p_y + A_z p_z + A_a p_a + \dfrac{A_z}{2} p_b + \dfrac{A_y}{2} p_c, \\[2mm] \sigma_l = p_x + \dfrac{A_y - 1}{m} p_y + \dfrac{A_x - 1}{m} p_z + \dfrac{A_a - 1}{m} p_a + \dfrac{A_z + m - 1}{2m} p_b + \dfrac{A_y + m - 1}{2m} p_c, \\[2mm] \tau_{tl} = F_b P_b + F_c p_c. \end{array} \right\} \tag{2.17}$$

The stress coefficients A_y, A_z, A_a, F_b and F_c, appearing in Eq. (2.17), are determined by the photoelastic experiments shown in Table 1, and p_x, p_y, $\cdots$, p_c are calculated from the magnitudes and directions of p_1, p_2 and p_3, using Eq. (2.7).

Accordingly, at Point P on the wall surface,

$$\sigma_t = A_x \sigma_x + A_z \sigma_z = A_z p_b. \qquad \text{(Since } A_x = 0.\text{)}$$

On the other hand, since the wall surface is parallel to the x-axis, the magnitude of σ_t, caused by a loading p_b in the b-direction is equal to that caused by a loading in the $\bar{b}$-direction. Therefore the magnitude of σ_t, when a model is subjected to loadings in both b and $\bar{b}$-directions simultaneously with the same intensity p_b, is given by

$$\sigma_t = 2A_b p_b.$$

Thus we get Eq. (2.13).

** Let the $\bar{a}$-axis be the bisector of the z-axis and the minus side of the y-axis. The stress component σ_t caused by loadings with an intensity of p_a in the a and $\bar{a}$-directions simultaneously is equal to that caused by loadings with the same intensity in the y and z-directions simultaneously, whereas σ_t at a point caused by a loading in the $\bar{a}$-direction is equal to σ_t at the symmetrical point by a loading with the same intensity in the a-direction. Consequently we obtain Eq. (2.15).

Table 1

Stress coefficients	Two-dimensional photoelastic experiments, loading a model in	Three-dimensional photoelastic experiments, loading a model in	Remarks
A_y A_z A_a	y–direction z–direction a–direction		Consider Eq. (2.15).
F_b F_c		b–direction c–direction	

In the special case where the direction of the axis of a shaft or a level coincides with the direction of p_1, namely the x–axis coincides with the x'–axis,

$$l_1 = 1, \quad l_2 = l_3 = m_1 = n_1 = 0,$$

and therefore, according to Eq. (2.7), we have

$$p_b = p_c = 0.$$

Thus the components of stress are given by the following equations:

$$
\left.
\begin{aligned}
\sigma_t &= A_y p_y + A_z p_z + A_a p_a, \\
\sigma_l &= p_x + \frac{A_y - 1}{m} p_y + \frac{A_z - 1}{m} p_z + \frac{A_a - 1}{m} p_a, \\
\tau_{tl} &= 0.
\end{aligned}
\right\}
\qquad (2.18)
$$

We only have to know, in this case, the three stress coefficients A_y, A_z and A_a from two-dimensional photoelastic experiments.

Photoelastic experiments

In the manner described above, the stress was investigated around a shaft or level whose cross section is a square or rectangle with rounded corners. In order to compare the results of experiment with those of theory, the stress around a circular shaft or level was also found in the same way.

Two-dimensional photolastic experiments were carried out to determine A_y, A_z and A_a, which are given by dividing the value of σ_t obtained experimentally by the intensities of loading in the y, z and a–directions respectively. The details of the two-dimensional photoelastic experiments will be omitted here for they are well known.

Three-dimensional photoelastic experiments were carried out to determine F_b and F_c. The shape and size of the models for these experiments are illustrated in Fig. 4. The models were loaded uniformly, with an intensity of about 1.5 kg/cm², by dividing the surface into thirty-six squares and loading them uniformly with the same weights, and the stress patterns were fixed by heat
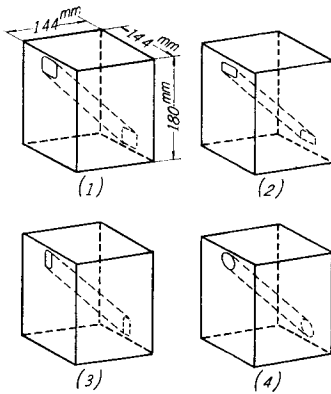
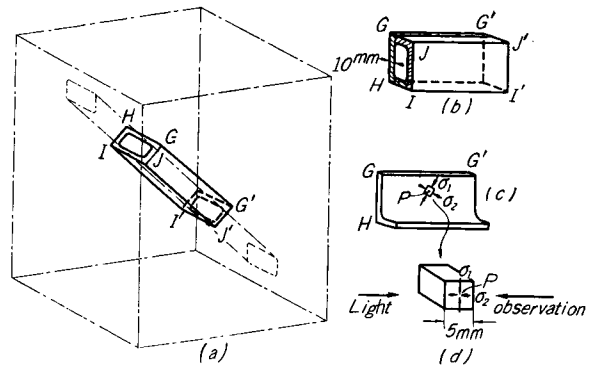Fig. 4. Models for three-dimensional photoelastic experiments.

Fig. 5. Cutting a model in order to determine the principal stresses at Point P.

treatment. Then the models were cut into a number of small pieces for observation, as shown in Fig. 5.

The determination of F_b and F_c at any point P on the wall of an opening was practised in the following manner. At first, a flat piece was cut out from the wall of an opening around Point P (Fig. 5 (a,b,c)). Projecting plane polarized light normal to the wall at Point P, isoclinics were observed, from which the directions of principal stresses were determined. (Fig. 5 (c)). Then, as shown in Fig. 5 (d), a small square prism, 5 mm × 5 mm in cross section, was cut out of the flat piece around Point P, and by projecting circular polarized light in the direction perpendicular to one of the principal stresses, say σ_1, and the n-direction, the fringe order was determined, from which the principal stress σ_1 was evaluated,

Table 2 Values of stresss coefficients

Cross Section	Stress Coefficients	P0 / P12	P1 / P13	P2 / P14	P3 / P15	P4 / P16	P5 / P17	P6 / P18	P7 / P19	P8 / P20	P9 / P21	P10 / P22	P11 / P23
(section 1)	A_1	2.16	2.22	2.75	1.50	-0.60	-0.97	-1.00	-0.97	-0.60	1.50	2.75	2.22
	A_2	-1.00	-0.97	-0.60	1.50	2.75	2.22	2.16	2.22	2.75	1.50	-0.60	-0.97
	A_3	0.57	1.39	3.00	5.40	3.00	1.39	0.56	-0.05	-0.95	-2.40	-0.95	-0.05
	F_b	0	±0.11	±0.19	±0.05	∓0.62	∓0.46	∓0.40	∓0.46	∓0.62	±0.05	±0.19	±0.11
	F_c	∓0.40	∓0.46	∓0.62	±0.05	±0.19	±0.11	0	∓0.11	∓0.19	∓0.05	±0.62	±0.46
(section 2)	A_1	1.68	1.79	2.35	0.60	-0.45	-0.90	-1.00	-0.90	-0.45	0.60	2.35	1.79
	A_2	-1.00	-0.99	-0.50	2.18	3.38	2.95	2.78	2.95	3.38	2.18	-0.50	-0.99
	A_3	0.34	1.16	2.94	4.55	4.13	2.99	0.86	0.13	-1.26	-1.69	-1.15	-0.41
	F_b	0	±0.21	±0.29	∓0.19	∓0.95	∓0.76	∓0.70	∓0.76	∓0.95	∓0.19	±0.29	±0.21
	F_c	∓0.25	∓0.25	∓0.44	∓0.01	±0.12	±0.11	0	∓0.11	∓0.12	±0.01	±0.44	±0.25
(section 3)	A_1	2.78	2.95	3.38	2.18	-0.50	-0.99	-1.00	-0.99	-0.50	2.18	3.38	2.95
	A_2	-1.00	-0.90	-0.45	0.60	2.35	1.79	1.68	1.79	2.35	0.60	-0.45	-0.90
	A_3	0.86	2.99	4.13	4.55	2.94	1.16	0.34	-0.41	-1.15	-1.69	-1.26	0.13
	F_b	0	±0.11	±0.12	∓0.01	∓0.44	∓0.25	∓0.25	∓0.25	∓0.44	∓0.01	±0.12	±0.11
	F_c	∓0.70	∓0.76	∓0.95	∓0.19	±0.29	±0.21	0	∓0.21	∓0.29	±0.19	±0.95	±0.76

taking into account the photoelastic sensitiveness determined from test pieces which were produced with the same material under the same heat treatment at the models. The determination of fringe orders requires some inventive means. From the magnitudes and directions of the principal stresses thus obtained, the component of shearing stress τ_{tl} at Point P was calculated. Dividing it by the intensity of loading in b or c-direction, F_b or F_c was obtained. Table 2 shows the values of the five stress coefficients A_y, A_z, A_a, F_b ane F_c, thus obtained, for a shaft or level whose cross section is a square, a lying rectangle or standing rectangle with rounded corners.

In order to examine the accuracy of the determination of stress coefficients from three-dimensional photoelastic experiments, the values of A_b and F_b obtained from these experiments are compared with those calculated theoretically using Eq. (1. 25) in Table 3.

Table 3. Comparison of the values of stress coefficients concerning a circular shaft or level obtained experimentally with those obtained theoretically.

Stress Coefficients ●		Values of stress coefficients at points whose angles of deviation θ are						
		0°	15°	30°	45°	60°	75°	90°
A_b	Theoretical	−0.50	−0.37	0	0.50	1.00	1.37	1.50
	Experimental	−0.60	−0.39	0.09	0.51	1.03	1.53	1.80
F_b	Theoretical	1.00	0.97	0.87	0.71	0.50	0.26	0
	Experimental	1.00	0.95	0.82	0.62	0.28	0.08	0

We see, from this table, that it is fairly difficult to obtain accurate values of stress coefficients from the experiments. Probably, the error is caused by the error in making models, by the thickness of slices through which isochromatics are observed, and so on.

Discussion

Let us assume that a circular inclined shaft is excavated in the ground in which $p_1=p_2=kp_3$ and p_3 is vertical, and denote the center points of the side wall and the roof with A and B respectively. The variations in σ_θ, σ_ζ, $\tau_{\theta\zeta}$ at Points A and B as well as the magnitudes and directions of principal stresses at Point A with the angle of inclination ϕ of the inclined shaft are investigated according to Eq. (1. 25), and assuming that Poisson's number for the ground is 4. They are as shown in Fig. 6 (a), (b), (c). For $\phi=0$, the inclined shaft becomes a level, while for $\phi=90°$, it becomes a vertical shaft.

From Fig. 6 it is seen that the greatest stress appearing on the wall is maximum when $\phi=0$, while it is minimum when $\phi=90°$.
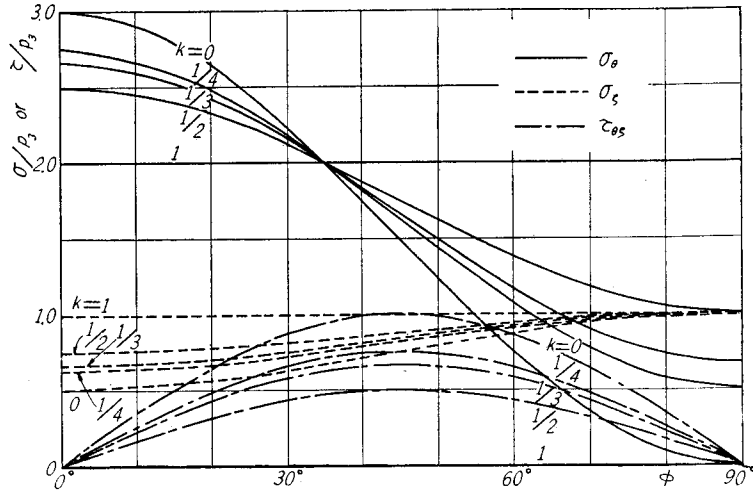
Fig. 6 (a).   Relations between the stress components σ_θ, σ_ζ, $\tau_{\theta\zeta}$ at Point A and the angle of inclination ϕ.
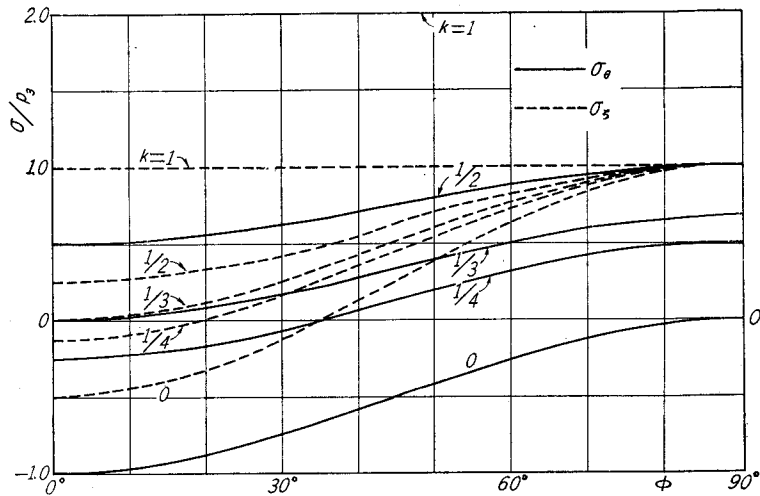
Fig. 6 (b).   Relations between the stress components σ_θ, σ_ζ at Point B (principal stresses) and the angle of inclination ϕ.
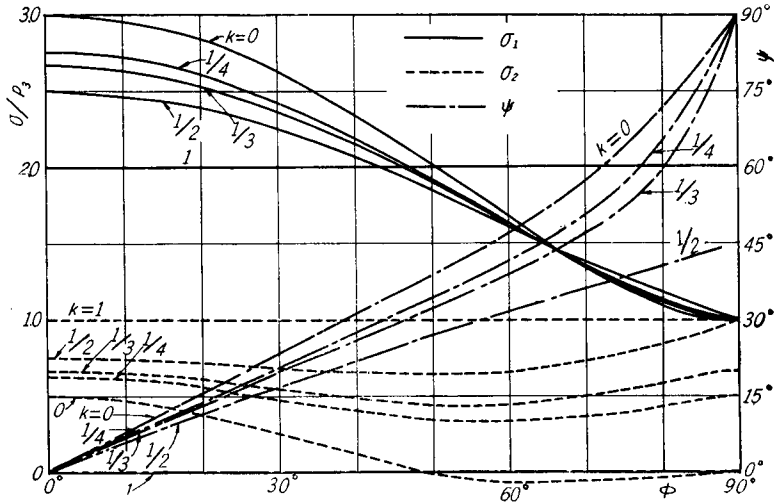
Fig. 6 (c). Relations between the magnitudes and directions of principal stresses at Point A and the angle of inclination ϕ, ψ being the angle of the smaller compressive principal stress measured from ζ-axis.

Now we proceed to discuss the stress concentration around a shaft or level in the case where the directions of all the principal stresses in the undisturbed ground deviate from the vertical or horizontal. Assuming that the principal stresses in the undisturbed ground are as shown in Fig. 7, the distributions of principal stresses on the wall of a vertical shaft, an inclined shaft ($\phi = 15^{\circ}$) and a level are illustrated in Fig. 8 (a) ~ (d). In these figures, the magnitudes and directions of principal stresses are plotted on the development of the wall surface, the positive direction of the axis of the shaft or level being directed upwards. (a), (b), (c) and (d) of Fig. 8 correspond to shafts or levels with a circular, square and two rectangular (lying and standing) cross sections respectively. Fig. 8(a) is based on the theoretical stress, while Fig. 8 (b), (c) and (d) on the experimental stress. In all cases, Poisson's number for the ground is assumed to be 4. Points $P_0, P_1, \cdots,$ P_{12} on the abscissa in Fig. 8 (b), (c)
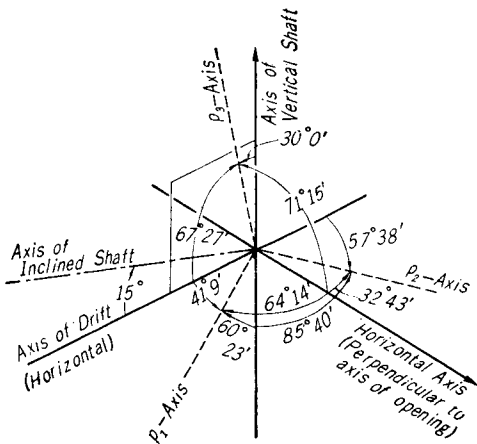

Fig. 7. An example of state of stress in the undisturbed ground ($p_1 = p_3/4$, $p_2 = p_3/3$).
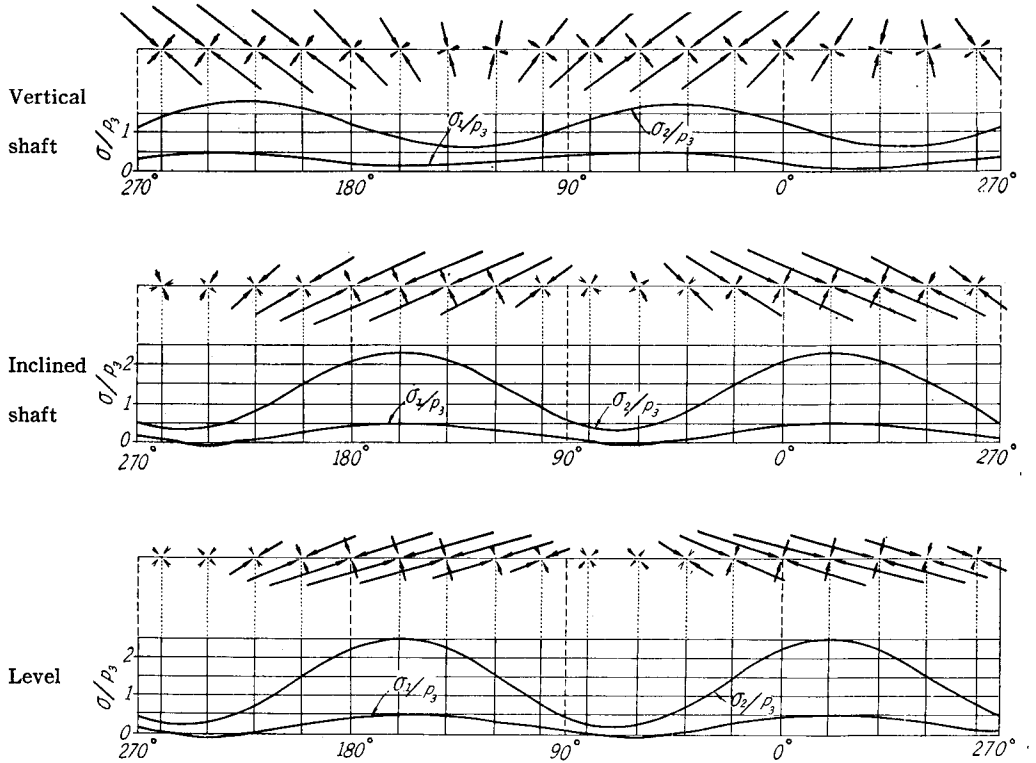
Vertical shaft

Inclined shaft

Level

Fig. 8 (a). The distributions of principal stresses on the wall of a vertical shaft, an inclined shaft ($\phi=15°$) and a level, with a circular cross section, which are made in the ground whose stress state is as shown in Fig. 7.
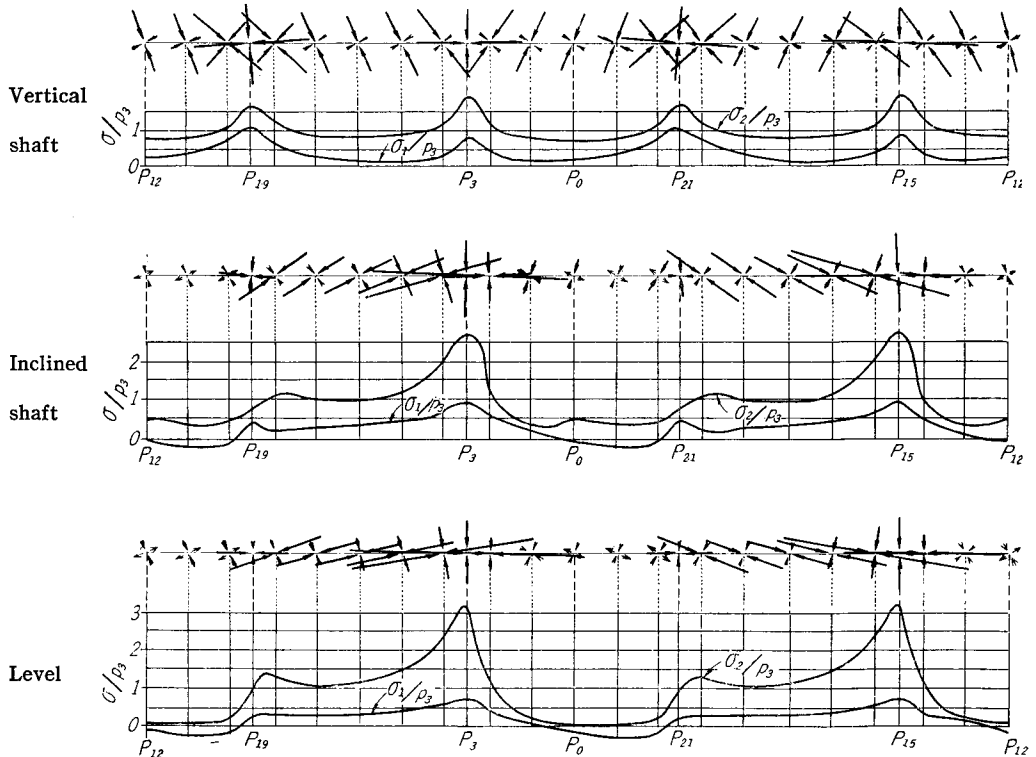
Vertical shaft

Inclined shaft

Level

Fig. 8 (b). The distributions of principal stress on the wall of a vertical shaft, an inclined shaft ($\phi=15°$) and a level, having a square cross section with rounded corners, which are made in the ground whose stress state is as shown in Fig. 7.

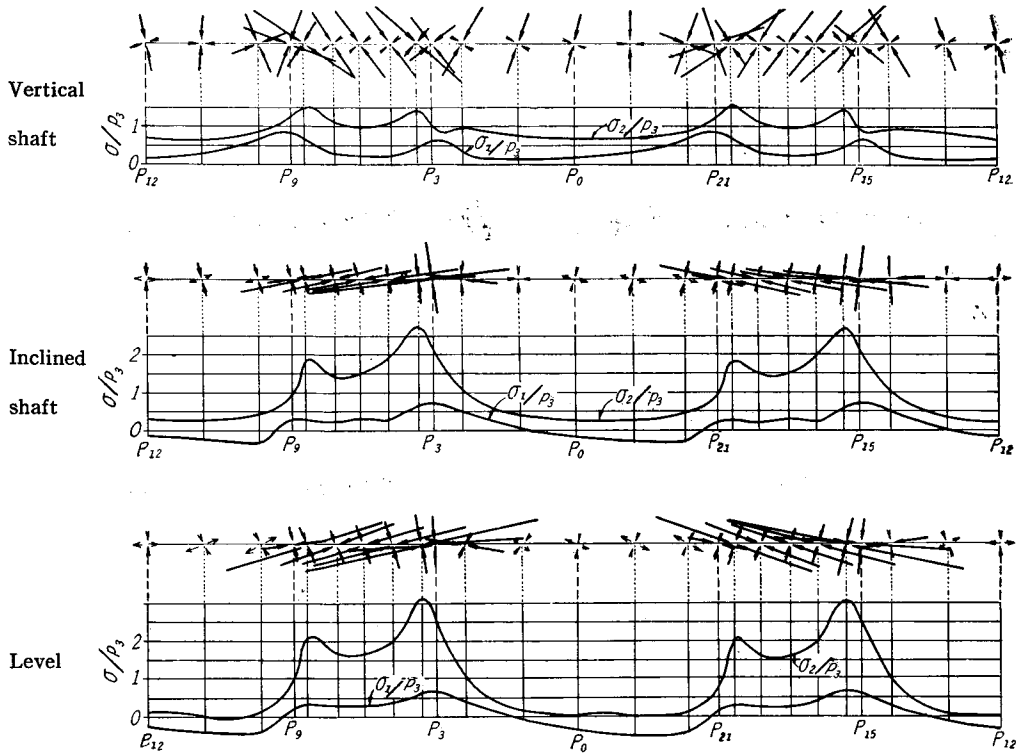Fig. 8 (c). The distributions of principal stresses on the wall of a vertical shaft, an inclined shaft ($\phi=15°$) and a level, having a lying rectangular cross section with rounded corners, which are made in the ground whose stress state is as shown in Fig. 7.
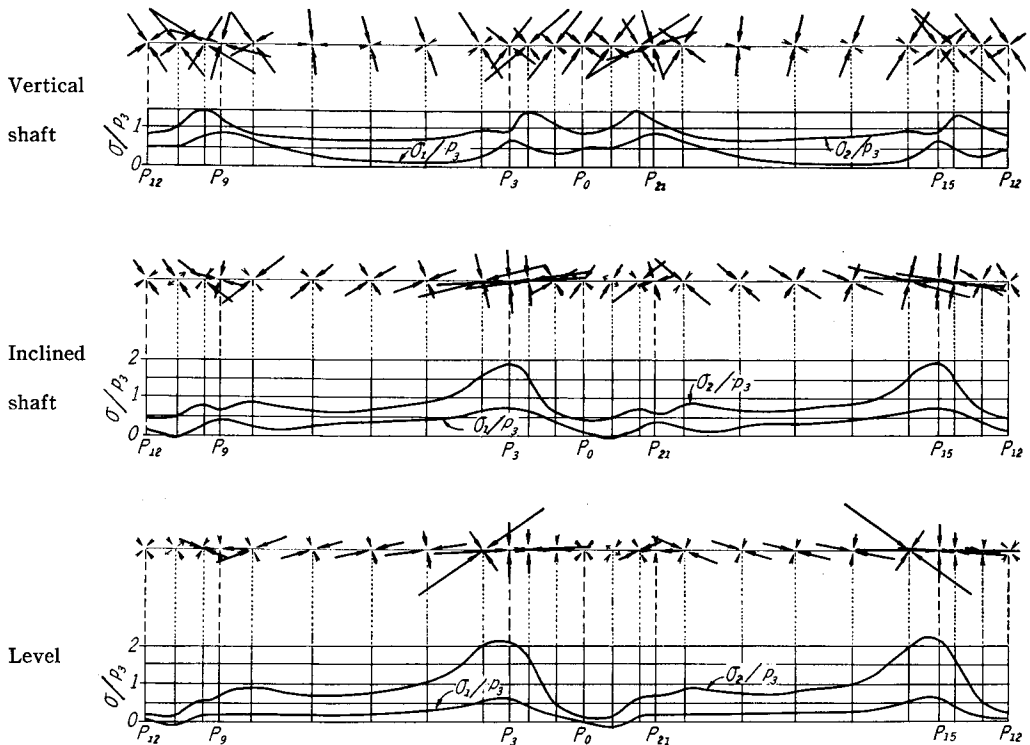

Fig. 8 (d). The distributions of principal stresses on the wall of a vertical shaft, an inclined shaft ($\phi=15°$) and a level, having a standing rectangular cross section with rounded corners, which are made in the ground whose stress state is as shown in Fig. 7.

and (d) correspond to those shown in Table 2. In Fig. 8 (a), however, the positions of points are expressed by the angle of deviation θ.

From Fig. 8, it is seen how the principal stresses on the wall deviate from the direction of the axis of the shaft or level (or from the direction perpendicular to it) with the deviation of that axis from the direction of one of the principal stresses in the undisturbed ground.

It seems that along the outline of the cross section, the maximum tensile stress (or the minimum compressive stress) may appear near the points which the plane containing p_3 (the greatest of p_1, p_2, p_3) and the axis of the shaft or level cuts the outline, whereas the maximum compressive stress may appear near the points where the plane perpendicular to the former cuts the outline. However the above mentioned rule becomes ambiguous when p_1 or p_2 is considerably large or when there are corners on the cross section, since the points of maximum stresses have a tendency to be drawn toward the corners.

The maximum compressive stress appearing on the wall is much affected by the directions of the maximum of the principal stresses in the undisturbed ground, so that the maximum stress can hardly be expressed by a simple rule. But it may not be a great mistake to say that the greatest stress in all cases is of about the same order as the greatest stress appearing in the case where the axis of the shaft or level is in the direction of p_1 or p_2.

Summary

The stress around underground openings is much affected by the state of stress in the ground in which the openings are made. The present paper treats the stress around a vertical shaft, an inclined shaft and a level, taking into account that the ground is in a three-dimensional stress state.

First the stress around a circular shaft or level is analyzed theoretically. Then, the general method of experimental analysis of the stress around a shaft or level is discussed, paying special attention to the evaluation of indeterminate stresses.

Secondly the stress around shafts and levels with a square and with two rectangular cross sections, all having rounded corners, is found by two-dimensional and three-dimensional photoelastic experiments. The results obtained are illustrated, from which the influence of the state of stress in the undisturbed ground upon the stress around a shaft or level is discussed.

References

1) N. Yamaguchi ; J. Inst. Civil Engr. Japan, **15**, 291 (1929).
2) H. Suzuki ; J. Inst. Mining and Metallurgical Engr. Japan, **65**, 118 (1949).
3) T. Sugihara ; J. Inst. Mining and Metallurgical Engr. Japan, **47**, 1176 (1931).
4) Y. Hiramatsu, Y. Oka and T. Kosumi ; J. Inst. Mining and Metallurgical Engr. Japan, **75**, 1080 (1959).